This is a postprint version of the following published document:

Feito, N., Diaz-Álvarez, J., López-Puente, J. & Miguelez, M. (2016). Numerical analysis of the influence of tool wear and special cutting geometry when drilling woven CFRPs. *Composite Structures, vol. 138*, pp. 285–294.

DOI: 10.1016/j.compstruct.2015.11.065

© 2015 Elsevier Ltd.

This work is licensed under a Creative Commons Attribution-NonCommercial-NoDerivatives 4.0 International License.

Numerical analysis of the influence of tool wear and special cutting geometry when drilling woven CFRPs

N. Feito [a], J. Diaz-Álvarez [b], J. López-Puente [c], M.H. Miguelez [a],*

[a] Department of Mechanical Engineering, Universidad Carlos III de Madrid, Avda. Universidad 30, 28911 Leganés (Madrid), Spain
[b] Department of Aerospace and Biomedical Engineering, Universidad Carlos III de Madrid, Avda. Universidad 30, 28911 Leganés (Madrid), Spain
[c] Department of Continuum Media and Structural Analysis, Universidad Carlos III de Madrid, Avda. Universidad 30, 28911 Leganés (Madrid), Spain

Keywords:
Tool wear
Woven CFRPs
FE modeling
Drilling

ABSTRACT

CFRPs drilling is a common process in the aerospace industry carried out prior to components assembly. Machining induced damage leads to significant percentage of component rejection. Damage extension strongly depends on drilling geometry and cutting parameters. Fresh drill geometry changes with cutting time due to the wear progression and the risk for hole quality is enhanced as cutting progresses. The influence of wear on hole quality has been analyzed in the literature using mainly an experimental approach.

Simulation of drilling process is an effective method that can be used to optimize drill geometry and process parameters in order to control hole quality and analyze the drill wear evolution. In this paper a finite element model for drilling woven CFRPs, reproducing both fresh and worn tools, is presented. Two different point angles considering fresh and honned edge were modeled. A progressive intra-laminar failure model based on the Chang and Chang model is considered. Cohesive elements allowed the analysis of inter-laminar damage (delamination). The model demonstrated its ability to predict thrust force and delamination for different values of feed rate and cutting speed. Model predictions show the influence of tool geometry (including variations induced due to wear) on delamination.

1. Introduction

Carbon fiber reinforced polymer composites (CFRPs) are increasingly used in industry, not only in aircraft structures but also in other sectors. The excellent mechanical properties and low weight of CFRPs together with fatigue and corrosion resistance make them a suitable option for high responsibility applications [1].

Woven CFRPs present enhanced strength to weight ratio, fracture toughness and corrosion resistance when compared to tape composite. The improved mechanical properties due to the architecture of the abrasive fibers, leads to poor machinability of woven composites.

Drilling operations do not allow direct observation since they are difficult to study in process. On the other hand, the efficiency of the machining operations involves important economic consequences for companies since increasing exigent cutting conditions are required to optimize productivity [2].

Drilling is one of the most common operations since it is required for further mechanical joining of the structural components [3]. CFRPs are susceptible to suffer drilling induced damage causing a significant percentage of workpiece rejection. The enhancement of drilling process ensuring hole quality is still a challenge [4].

The influence of the cutting parameters [5,6], the point angle [7–9] and the drill diameter [10] for different tool materials have been analyzed in the literature.

Feed rate seems to be the most influencing factor in delamination (increasing with this parameter). The effect of cutting speed is not clear and seems to have a cross effect with thickness and spindle speed. Davim et al. [5] showed that delamination increased with cutting speed during conventional drilling. However Gaitonde et al. [6] showed an opposite effect when drilling at high spindle speed in thin woven-ply CFRP composite laminates. Cutting speed shows much lower influence than feed rate.

The effect of drill geometry was demonstrated in Karnik et al. [7] and Feito et al. [8]. It was observed that increasing the point angle of twist drill bit during conventional and high speed drilling of woven-ply CFRP composite laminates, delamination was increased. However Heisel et al. [9] reported that the

* Corresponding author.
E-mail address: mhmiguel@ing.uc3m.es (M.H. Miguelez).

http://dx.doi.org/10.1016/j.compstruct.2015.11.065
0263-8223/© 2015 Elsevier Ltd. All rights reserved.

delamination at the entry was decreased with the point angle. The increment of drill diameter also showed large contribution on delamination as it was proved by Tsao and Hocheng [10].

Geometrical modifications due to wear progression also influences resultant surface quality and delamination damage. Main wear mechanism in conventional drilling was identified to be abrasion (see for instance Mayuet et al. [11]) due to the presence of abrasive the fibers. Although abrasion is dominant, also adhesion was identified during the study. In this case exit delamination was observed to increase with wear progression.

For high speed drilling, chipping was observed at the first stages of drilling process (Rawat et al. [12]), following by abrasion and adhesion as cutting time progresses. This study also proved that abrasive wear on the flank face of the primary cutting edge was stronger than the wear at the rake face.

Tool wear also affects the cutting forces. It was reported in [13] that high feed rate increases the tool wear and consequently the thrust force. This fact is independ of the tool coating. Torque has demonstrated less sensibility to wear evolution than thrust force [13].The authors also studied the influence of worn tools in cutting forces and delamination in [8]. Similar conclusions were derived: experimental results showed that crossed effect of feed rate and worn tool increases appreciably the thrust force. Concerning delamination, while entry damage diminished with wear progression, exit damage was enhanced.

The change of the geometry due to abrasion leading to cutting edge rounding (CER) was analyzed for different geometries by Faraz et al. [14]. Positive correlation was found between both delamination and cutting forces and the cutting edge roundness.

Despite the interest of the experimental approaches, finite element (FE) analysis completes the study of drilling performance, since modeling is a powerful tool that can be used to support testing, avoiding technical problems and elevated cost. FE analysis allows controling all variables that take part during the machining process and uncoupling the influencing parameters. A recent review gives an overview of machining models of different types of composites [15].

There are few works in the literature focusing on numerical modeling of composite drilling. Most papers presenting numerical modeling of composite cutting focus on orthogonal cutting due to its simplicity. Some examples of the modeling strategies and material modeling used in scientific literature for two dimensional (2D) approach to simulation of orthogonal cutting of composites can be found in [16–19]. 2D approaches only allow the simulation of unidirectional composite; moreover delamination cannot be study. To solve the problem of delamination in orthogonal cutting 3D modeling was introduced to allow reproducing different stacking sequences [20,21]. This model also was used to evaluate the validity of the assumptions involved in the formulation of 2D approaches. Focusing on current drilling operations, 3D modeling is required. Different approaches can be found in the literature. First models developed were based on a simplified quasi-static three-dimensional (3D) simulation of drilling, which considers the drill as a punch. Some examples of this approach were used by Durao et al. in [22,23] for CFRPs materials and Singh et al. [24] in order to study drilling of glass fiber reinforced polymer composites (GFRPs). Main objective was obtaining a relation between delamination and the applied thrust force that seems to be one of the governing factor in the generation of out-of-plane failure during drilling as reported also in Upadhyay et al. [25]. These models were also used to study the influence of the drill point angle on delamination damage [22]. It was observed that 90° drill point angle gives better results than those obtained with 104° and 118°.

Further improvements of drilling simulation have led to the development of 3D complex drilling models for CFRPs. Drilling was successfully reproduced including drill penetration in the workpiece, material failure and chip removal [26,27]. Modeling of drilling processes involves elevated difficulty because of the need to simulate drill rotation and feed using both damage and erosion criteria involving high computational cost. The authors presented a recent work focusing on the comparison of simplified and complex models of composite drilling [28]. It was proved that simplified model can save computational time due to its simplicity while overestimates the prediction of damage.

This work presents a new 3D FE analysis accounting for the effect of worn geometry when drilling woven materials. Also the effect of drill point angle and cutting parameters with new and worn tool was analyzed. The model has been validated in comparison with experimental work in terms of thrust force and delamination extension, showing good accuracy.

The present work is structured as follows. Firstly, experimental work required for model validation is presented in the next section. Numerical work providing details of constitutive and contact modeling is given in the third section. Model validation and results achieved with simulations are presented in the fourth section, including mechanistic model derived from the numerical simulations. Finally conclusions are stated in the last section of the paper.

2. Experimental work

2.1. Workpiece material

The specimens were made using plain woven prepregs with AS4 fiber and 8552 epoxy matrix, commercially denoted AGP193-PW by its manufacturer Hexcel Composites. This composite, commonly used in aerospace industry, was cut in pieces of 120 mm × 29 mm in order to introduce them in a confining device specially designed to avoid dispersion of the fiber chip (see previous work of the authors [8] providing detailed description of the confining device) The laminate was composed of 10 plies with bidirectional orientation of the fibers, with thickness equal to 2.2 mm. The characteristics and mechanical properties of this material are presented in Table 1 where ρ is density; E_i is the elastic modulus in the direction i, ν_{ij} is the Poisson coefficient, G_{ij} is the elastic modulus in shear directions, X_t, Y_t and S_t are the maximum tensile stress in longitudinal and shear directions respectively, X_c and Y_c are the maximum compressive stress in longitudinal directions and ε_l is the critical strain.

2.2. Drill characteristics

Three different drill bits were selected. The first one was a conventional twist drill with different point angles (90° and 118°). Fresh drill, corresponds to the geometry given by the tool manufacturer (Fig. 1 case A). The second drill bit was a worn tool with honed edge wear with length equal to 0.05 mm. Honed edge is a wear mode, consequence of wear mechanisms observed when

Table 1
Mechanical properties of carbon–epoxy woven laminate [29].

Property	Value
ρ	1570 kg/m^3
$E_1 = E_2$	68 Gpa
E_3	10 Gpa
υ_{12}	0.22
$X_t = Y_t$	880 Mpa
$X_c = Y_c$	880 Mpa
S_t	96 Mpa
$\varepsilon_1 = \varepsilon_2$	0.025
ε_3	0.05

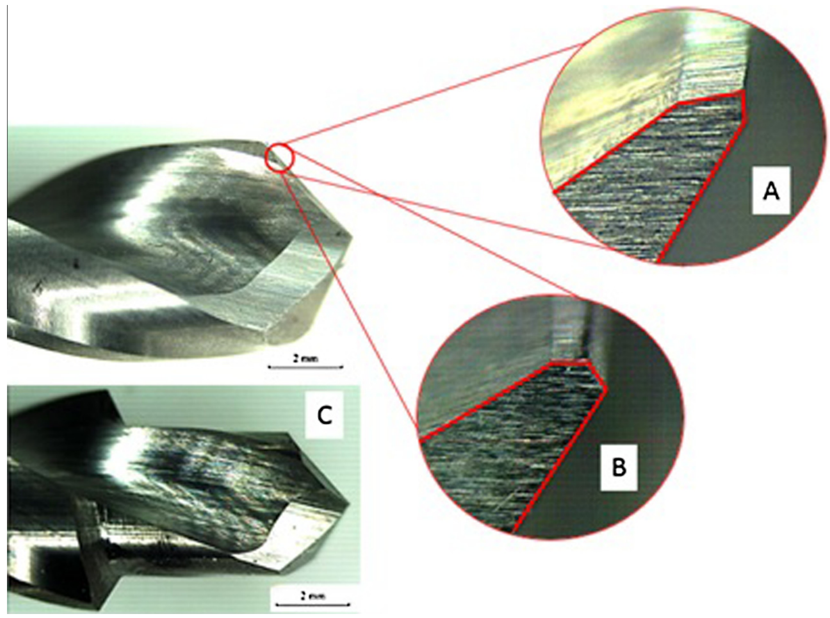

Fig. 1. Drill bit geometries for fresh drill (A), honed edge drill (B) and step drill (C).

drilling CFRP, as it was stated in a previous work of the authors [8]. In order to control the worn geometry, it was artificially generated through a grinding process by the manufacturer GUHRING [30] (Fig. 1 case B). Finally, the third case was a step twist drill with an initial diameter equal to 4 mm. The step had a length equal to 6.6 mm (Fig. 1 case C). In all cases the nominal diameter of the drill was 6 mm.

2.3. Machining tests

Both thrust force and torque were measured during dry drilling tests using a rotating dynamometer (Kistler 9123C). A machining center (B500 KONDIA) was equipped with a confining system with a supporting back plate previously drilled with hole diameter equal to 10 mm (see Fig. 2). The aim was avoiding chips spreading combining the confining box with a vacuum to remove them. Cutting parameters are summarized in the Table 2.

The delamination factor (F_d), defined as the ratio between the maximum diameter of delaminated area and the nominal hole diameter, was calculated through the measurement of diameters obtained from images taken with an optical stereo microscope (Optika SZR).

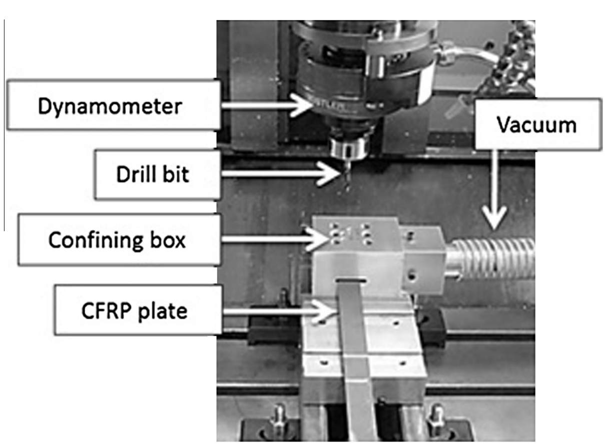

Fig. 2. Set-up device for drilling tests showing confining box.

Table 2
Cutting parameters used in drilling tests: feed rate (*f*) and cutting speed (*V*).

Parameter	Range		
f [mm/rev]	0.05	0.1	0.15
V [m/min]	25	50	100

3. Numerical modeling

The model presented in this work, was able to reproduce drilling of woven composite including chip removal. The FEM code ABAQUS/Explicit [31] was used to perform the numerical simulations. The complete movement of the drill including spindle speed and feed rate was simulated. In a previous work of the authors [28] it was presented the main advantages and drawbacks of this complex model when compared with simplified models assuming drilling as a punching process. Since the aim of this paper is simulating the effect of tool geometry changes induced by wear, the development of complete model including both rotary and feed movement and chip removal is required.

The scheme of the model developed is presented in the Fig. 3. The displacement of the workpiece in *Z* direction was restricted at the base except for the zone inside a circumference with 10 mm diameter where it is free. This boundary condition reproduces the effect of the supporting back plate used in the experiments.

3.1. Drill and workpiece behavior

The drill was assumed to be rigid with nominal diameter equal to 6 mm.

The woven laminate was modeled as an orthotropic elastic material until failure. This approach has been successfully implemented by López-Puente et al. [32] to simulate dynamic loading (impact) in the same material. Both intra-laminar and inter-laminar damage mechanisms were defined. The first one was implemented by means of a user subroutine (VUMAT). The second

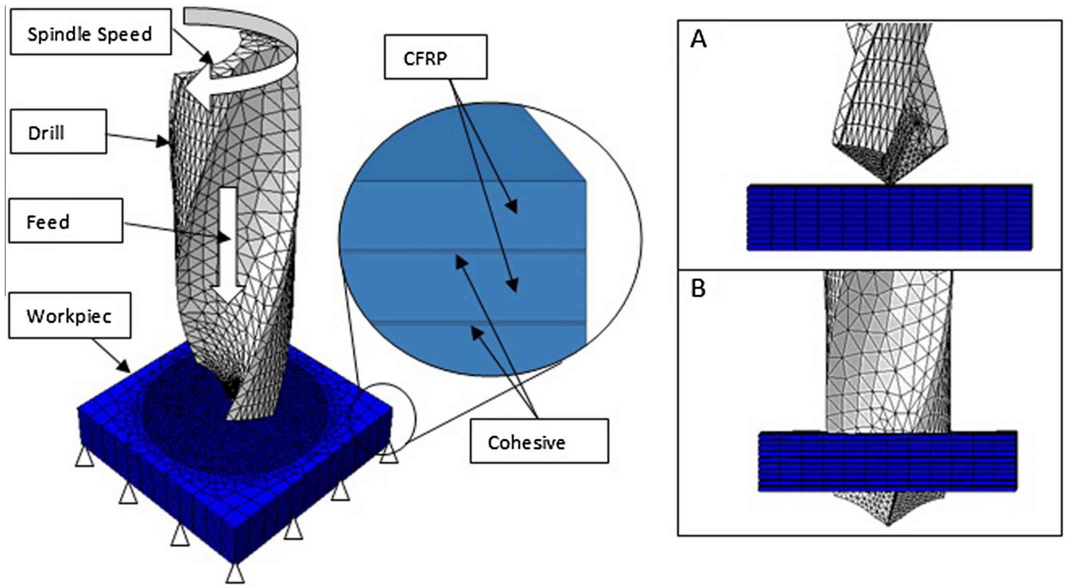

Fig. 3. Scheme of the complete model. Drill entrance simulation; (A) initial and (B) final drill position.

one was achieved using cohesive elements. This implementation of different failure mechanisms has been used in previous work of the authors [29] modeling impact processes and also drilling [28].

The fiber and matrix damages were defined in the Eqs. (1)–(3) where the damage variables d_{ij} (stress dependent) range from 0 (undamaged) to 1 (fully broken). When the failure criterion is reached the stress components involved in the failure definition (fiber or matrix failure) are set to zero. To control the element erosion, strain tensor is calculated after each time increment. When one of the components reaches a critical value, the element is removed.

In woven laminates, fibers are located in orthogonal in-plane directions (1 and 2). Eq. (1) describes the fiber failure (d_{ij} equal to 1) in both directions:

$$d_{f_1} = \begin{cases} \sigma_{11}/X_t & \text{if } \sigma_{11} > 0 \\ |\sigma_{11}|/X_c & \text{if } \sigma_{11} < 0 \end{cases} \quad d_{f_2} = \begin{cases} \sigma_{22}/Y_t & \text{if } \sigma_{22} > 0 \\ |\sigma_{22}|/Y_c & \text{if } \sigma_{22} < 0 \end{cases} \tag{1}$$

where σ_{11} and σ_{22} are the stresses in the warp and fill direction respectively, X_t and X_c are the strengths of the composite laminate in tension and compression for the warp direction, and Y_t and Y_c are the strengths in tension and compression for the fill direction.

On the other hand two different parameters are proposed corresponding to crushing matrix failure mode (d_{ij} equal to 1), the first one in the ply plane Eq. (2) and the other one in the through-thickness direction Eq. (3).

$$d_{m12} = |\sigma_{12}/S_{12}| \tag{2}$$

$$d_{m_3} = \frac{1}{4}\left(\frac{\sigma_{33}}{Z_c}\right)^2 + \frac{Z_c \cdot \sigma_{33}}{4S_{13}S_{23}} + \left|\frac{\sigma_{33}}{Z_c}\right| + \max\left[\left(\frac{\sigma_{13}}{S_{13}}\right)^2, \left(\frac{\sigma_{23}}{S_{23}}\right)^2\right] \tag{3}$$

where σ_{ij} are the components of the stress tensor, S_{12}, S_{13} and S_{23} are the shear strengths in the three different planes and Z_c is the strength in the through-thickness direction under compression. The Eq. (3) is applied only when $\sigma_{33} < 0$.

The cohesive elements used to estimate delamination are based on a traction–separation law. The linear elastic behavior is required by means of the respective stiffness (K_{nn}, K_{ss} and K_{tt}). In this work, a quadratic nominal stress criterion for the damage initiation, similar to Eq. (4), was selected where t_n, t_s and t_t are the strengths of the cohesive interface in the normal and in shear directions respectively. Eq. (4) is applied if one of conditions on Eq. (5) is reached, where Z_t is the laminate strength under tension in the through thickness direction.

$$\left(\frac{\sigma_{33}}{t_n}\right)^2 + \left(\frac{\sigma_{13}}{t_s}\right)^2 + \left(\frac{\sigma_{23}}{t_t}\right)^2 \geqslant 1 \tag{4}$$

$$\sigma_{33} \geqslant Z_t \text{ or } \sqrt{\sigma_{12}^2 + \sigma_{13}^2} \geqslant S_{23} \tag{5}$$

The damage evolution follows a potential law type based on energies, see Eq. (6) where the parameter $\alpha = 1$; G_n, G_s and G_t are the released rate energy in the three aforementioned directions; and G_n^C; G_s^C and G_t^C are the critical values of the released rate energy. The values of these properties are shown in Table 3 [29].

$$\left(\frac{G_n}{G_n^C}\right)^\alpha + \left(\frac{G_s}{G_s^C}\right)^\alpha + \left(\frac{G_t}{G_t^C}\right)^\alpha \geqslant 1 \tag{6}$$

3.2. Drill geometry and workpiece meshing

Each ply was modeled at the zone around the diameter of the drill using solid elements C3D6R (wedge elements) with six nodes in order to minimize the dependence of the results with mesh orientation in the laminate plane. Just one element is located along the ply thickness. Minimum element size was 0.2 mm around the penetration zone. Far from to the drill entrance zone hexagonal elements C3D8R with 8 nodes and reduced integration were used, with minimum element size around 1 mm. Delamination is modeled by means of cohesive elements. Small thickness was assigned to the interface (5 microns) in order to improve numerical behavior when high deformations occur during calculation. Meshing strategy in the interface plane 1–2 was the same as that used in the ply, with one element along the thickness (direction 3).

Table 3
Parameters for the cohesive interface [29].

K_n	$K_{ss} = K_{tt}$	t_n	$t_s = t_t$	G_n	$G_s = G_t$
2 GPa/mm	1.5 GPa/mm	11 MPa	45 MPa	0.6 J/m^2	1.8 J/m^2

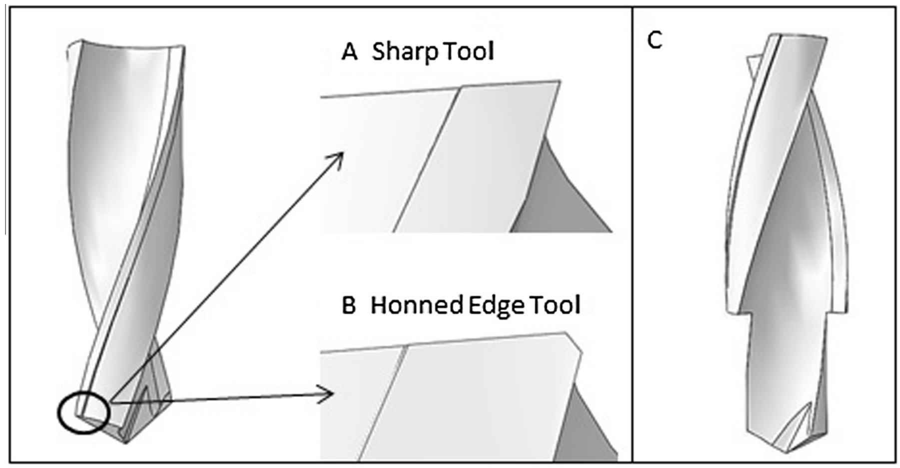

Fig. 4. Model of the geometries: helicoidal new (A), helicoidal honed (B) and step (C).

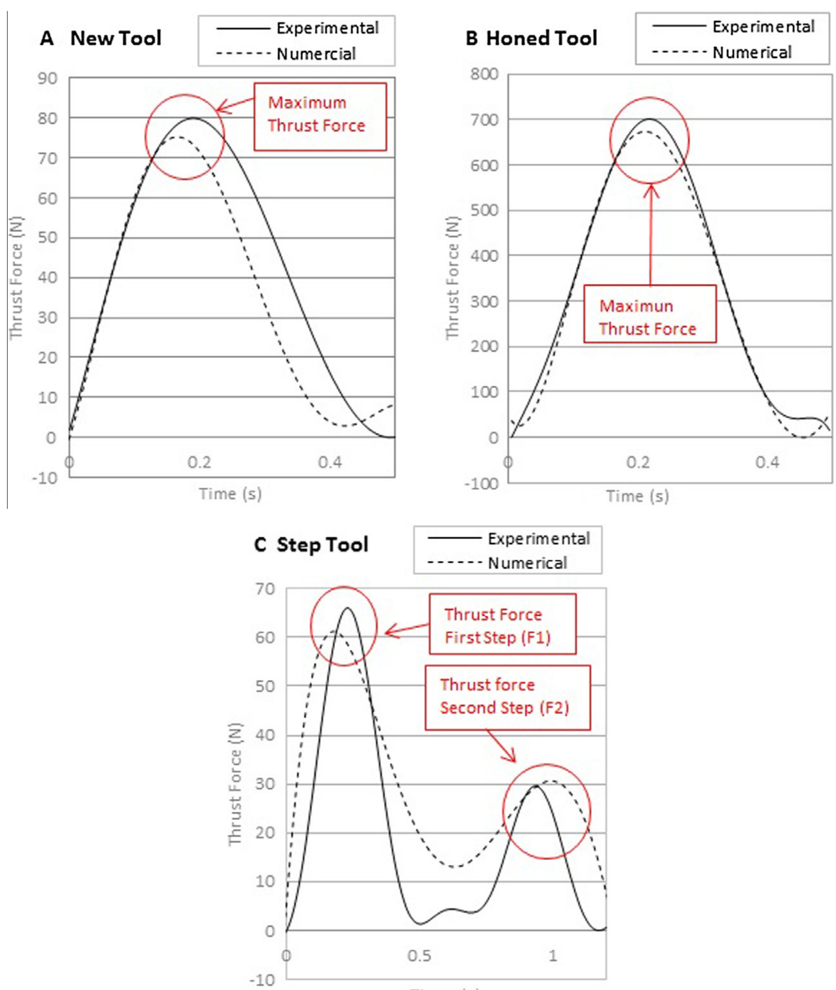

Fig. 5. Numerical and experimental thrust force evolution (A–C, different geometries considered in this study).

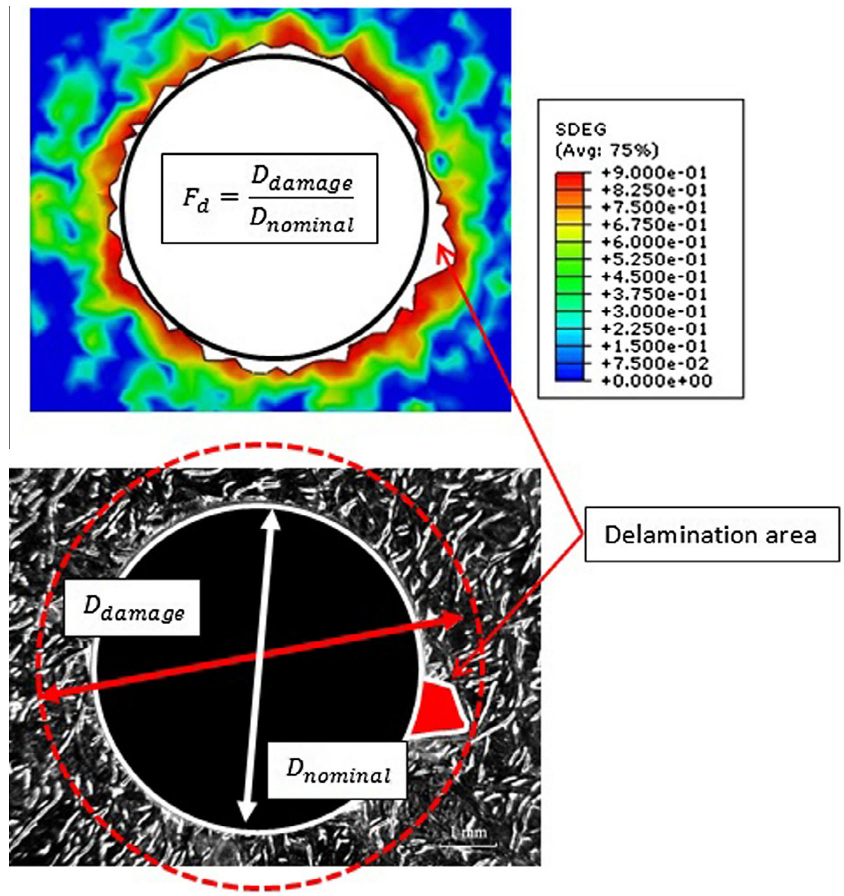

Fig. 6. Measured and predicted delamination (point angle: 90°; cutting speed: 100 m/min; feed rate: 0.10 mm/rev).

The geometry of the base model (corresponding to fresh tool, see Fig. 4A) was modified simulating the honed edge (see Fig. 4B). Also stepped drill geometry was simulated (Fig. 4C). Geometrical changes strongly affect thrust force and delamination, as it is demonstrated in next section.

4. Results

4.1. Model validation

Model validation was carried out comparing experimental and numerical results, in terms of thrust force and maximum delamination. Maximum thrust force (being the peak value of the thrust force evolution with cutting time) was obtained from the experimental measurement and the numerical simulations. Fig. 5 shows the trust force evolution with cutting time, showing good agreement between measured and predicted curves, both in terms of magnitude and shape. For these cases the cutting speed was equal to 100 m/min and the feed rate was equal to 0.010 mm/rev.

Fig. 6 shows predicted and measured exit delamination in the case of point angle equal 90°, cutting speed equal 100 m/min and feed rate equal 0.10 mm/rev. The measurement of the maximum diameter of delaminated area allows the calculation of delamination factor defined as $F_d = D_{\text{damaged}}/D_{\text{nominal}}$

Fig. 7 summarizes the numerical and experimental results (in terms of maximum thrust forces and exit delamination factor) for different geometries of the drill bit.

For the case of fresh drill (Fig. 5A), the maximum deviation in maximum thrust force and delamination factor were 7.7% and 2.6% respectively.

The model was modified to simulate worn geometry (Fig. 5B). In this case the drill point angle was 118° and the cutting speed was equal to 100 m/min. The difference between experimental and estimated values of thrust force were lower than 17%. Delamination factor presented maximum error around 3%.

Finally, the model was applied to the simulation of a special stepped drill bit geometry. Fig. 5C presents the results for this case. It can be observed very good predicted results in both thrust force and delamination factor with erors around 11.3% and 3.5% respectively.

In all cases analyzed, the model overestimates the delamination. This fact could be related to the characterization of the interface properties and the properties given to the cohesive elements (Eqs. (4)–(6), Table 3). These properties are obtained from [29], this study focuses on dynamic impact on the same woven CFRP. The properties required for cohesive elements do not account for strain rate dependence, but actually the response of the interface between plies could be influenced by the rate of the deformation.

4.2. Parametric analysis

Once the model was validated in different conditions, a parametric analysis was carried out in order to study the influence of the cutting parameters in the predicted thrust force and delamination factor.

Figs. 8 and 9 show the surface prediction for thrust force and delamination damage in the case of point angle equal 90° and 118° for new tool.

The feed is the most influencing factor both in thrust force and delamination. Although cutting speed has slight influence, the best

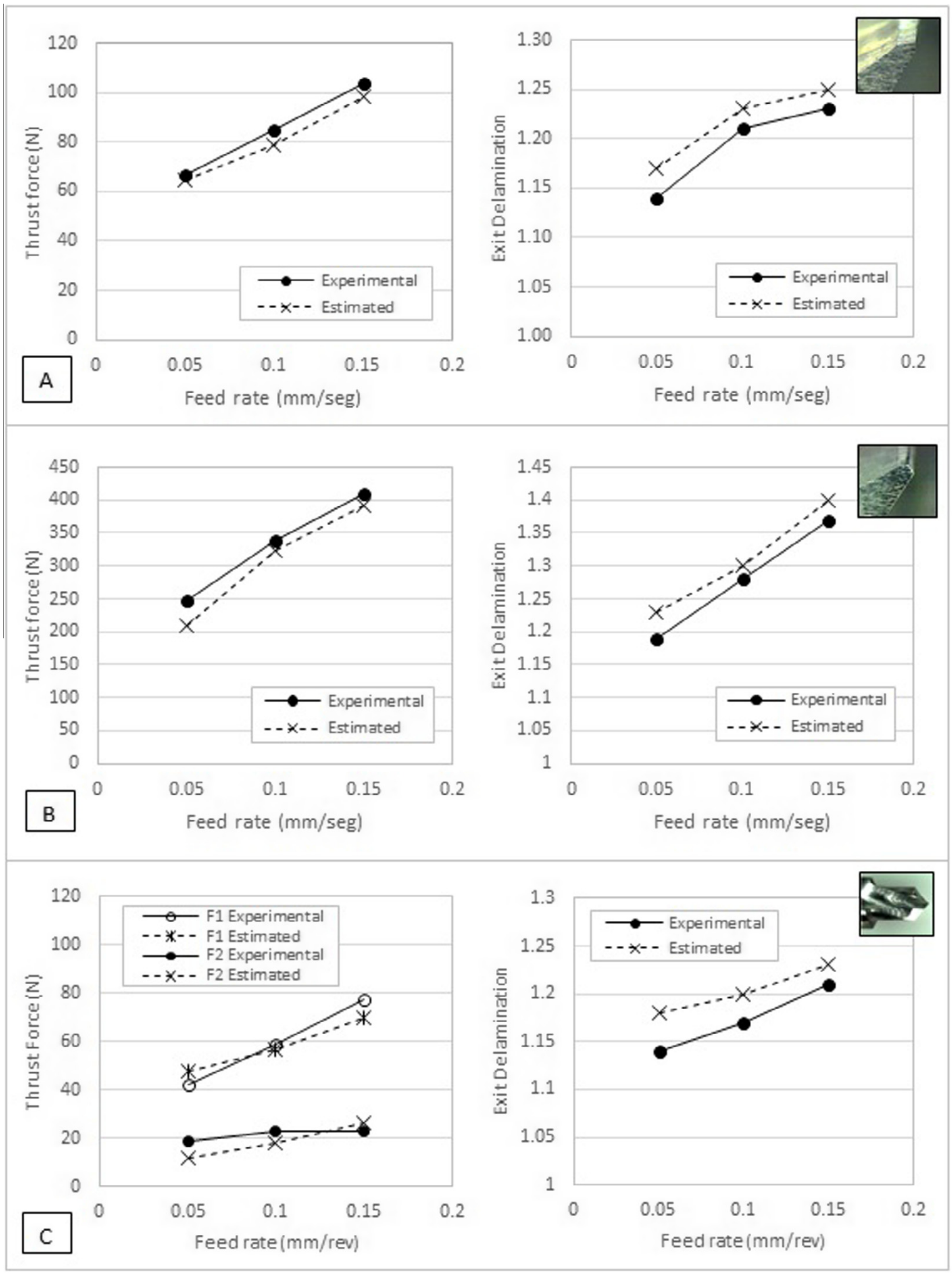

Fig. 7. Model validation for new drill bit with point angle equal 90° and cutting speed equal 25 m/min (A), for honed drill bit with point angle equal 118° and cutting speed equal 100 m/min (B) and for stepped geometry with cutting speed equal to 100 m/min (C).

combination in order to minimize damage seems to be high cutting speed and low feed rate since both force and delamination factor are decreased. These trends are in agreement with the experimental data found in the literature [6,8]. The use of the numerical model to obtain similar conclusions is interesting because of the possibility to apply the simulation to other materials, configurations and tools, avoiding expensive experimental work.

The numerical results obtained from the simulations allowed the adjustment of a mechanistic expression relating both thrust force and delamination factor to feed rate and cutting speed (see Table 4). With these equations it is possible to determine a diagram of evolution with both cutting parameters and estimate the values for a couple of cutting parameters (Fig. 10).

The simulations for the case of worn drill bit has been carried for the point angle equal to 118°. The model has been used to predict force and damage in the material changing the cutting speed. Numerical results are showed in Fig. 11. The influence of feed rate is lower than the observed with fresh tool, also the influence of cutting speed is almost negligible. The effect of worn geometry is dominant and thus the selection of proper parameters for damage minimization is difficult with worn tool. It is worth noting the elevated value of delamination factor even for low values of feed rate.

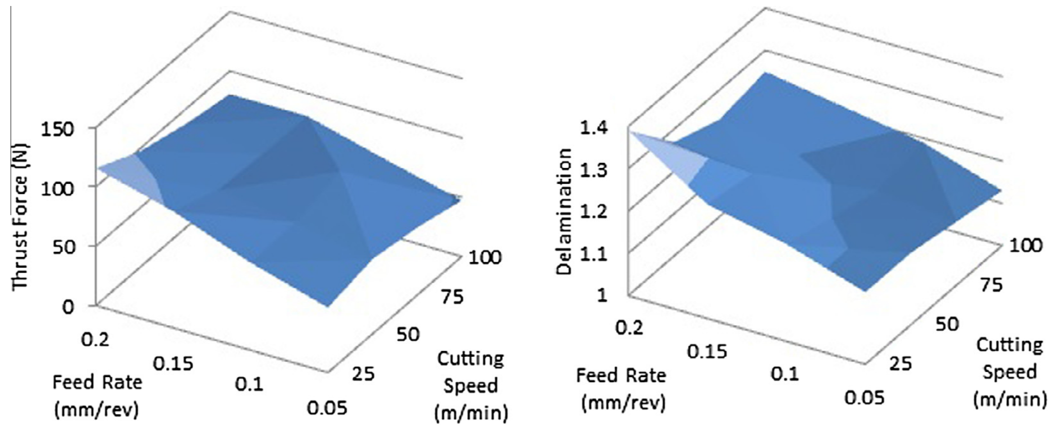

Fig. 8. Surface diagram for thrust force and delamination for a helicoidal drill bit (point angle = 90°).

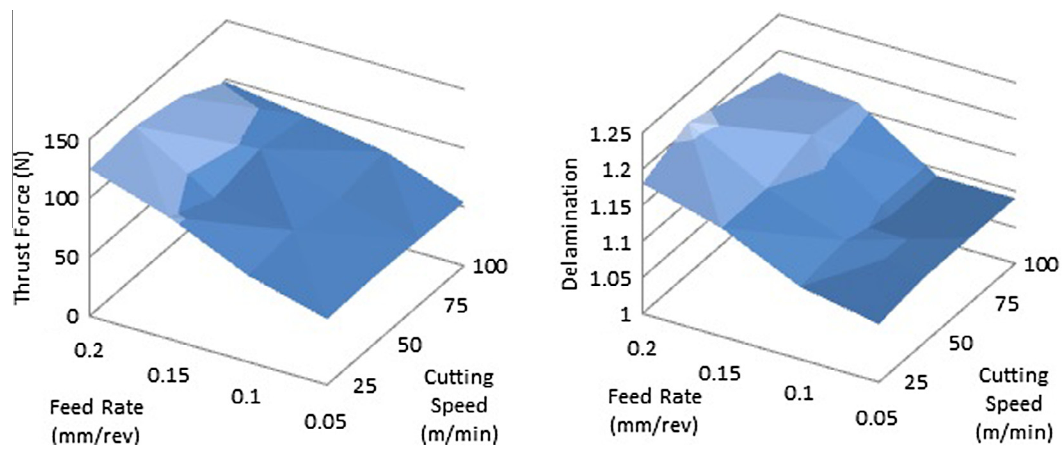

Fig. 9. Surface diagram for thrust force and delamination for a helicoidal drill bit (point angle = 118°).

Table 4
Prediction equations (thrust force and delamination) for worn tool at different cutting speeds.

Point angle	Prediction equation	R^2
90	$T_f(N) = -16.2629 + 1.8649 \cdot V + 962.9183 \cdot f - 14.9973 \cdot V \cdot f - 0.0143 \cdot V^2 - 948.675 \cdot f^2 + 0.1011 \cdot V^2 \cdot f$	0.94
	$D_f = 1.1837 + 0.0001 \cdot V - 0.195 \cdot f - 0.0166 \cdot V \cdot f - 0.00001 \cdot V^2 + 10.5 \cdot f^2 + 0.0003 \cdot V^2 \cdot f - 0.128 \cdot V \cdot f^2$	0.93
118	$T_f(N) = 71.92 - 0.9585 \cdot V - 271.63 \cdot f + 14.6184 \cdot V \cdot f + 0.0056 \cdot V^2 + 2592 \cdot f^2 - 0.0653 \cdot V^2 \cdot f - 37.736 \cdot V \cdot f^2$	0.96
	$D_f = 1.0981 - 0.001 \cdot V - 0.2075 \cdot f + 0.0146 \cdot V \cdot f + 8E\text{-}6 \cdot V^2 + 2.25 \cdot f^2 - 0.0001 \cdot V^2 \cdot f$	0.92

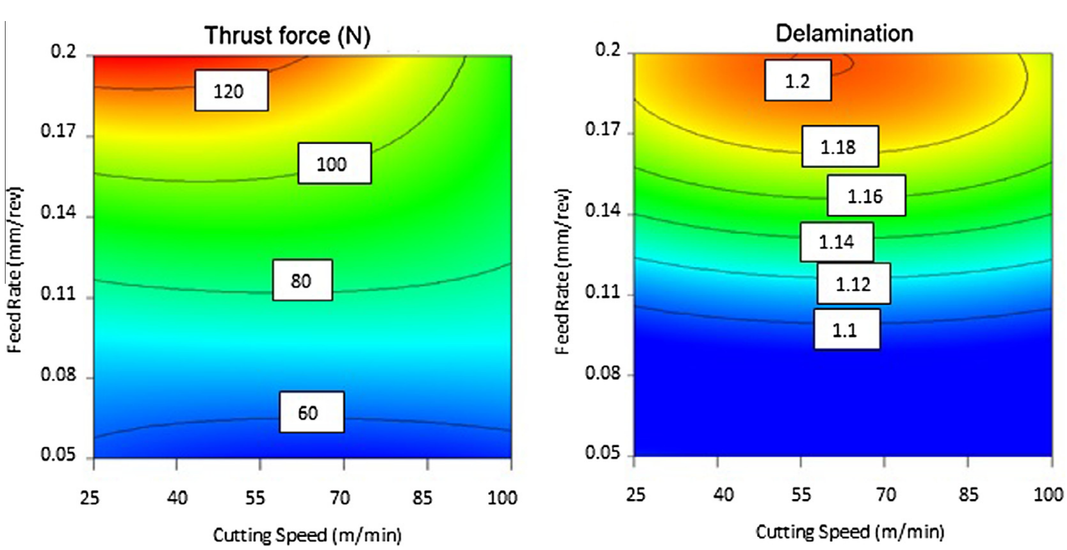

Fig. 10. Diagrams to estimate thrust force and delamination for a helicoidal drill bit with point angle equal 118°.

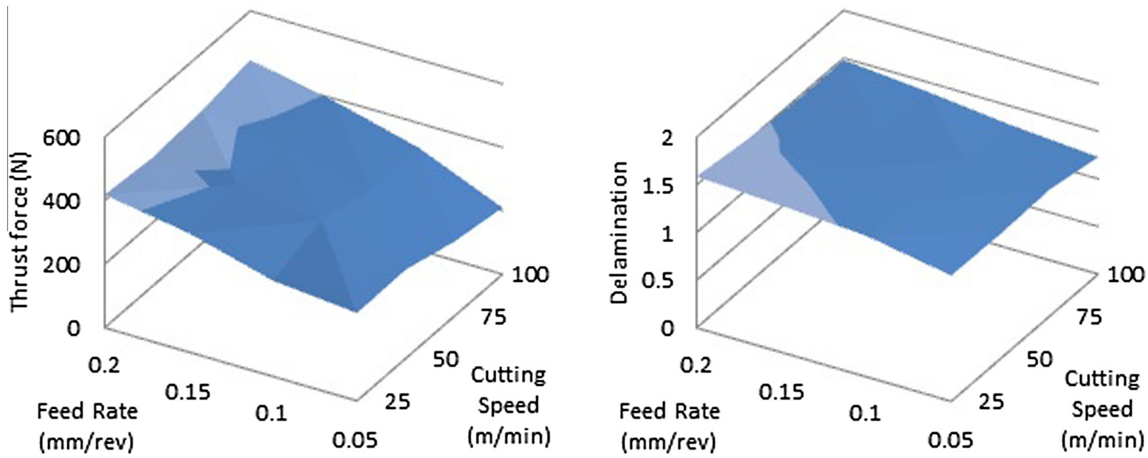

Fig. 11. Surface diagram for thrust force and delamination for honed edge drill bit.

Table 5
Prediction equations (thrust force and delamination) for step drill bit at different cutting speeds.

Point angle	Prediction equation	R^2
118	$T_f(N) = 272.0205 - 1.1143{\cdot}V + 634.463{\cdot}f + 8.1877{\cdot}V{\cdot}f$	0.93
	$D_f = 0.9725 + 0.0075{\cdot}V + 6.43{\cdot}f - 0.0941{\cdot}V{\cdot}f - 5.6\text{E-}5{\cdot}V^2 - 14{\cdot}f^2 + 0.00043{\cdot}V^2{\cdot}f + 0.152{\cdot}V{\cdot}f^2$	0.96

It can be observed that the predicted values for thrust force and delamination for the case of honned edge drill bit are higher than the estimated for new drill bit. This is in concordance with the experimental results published in a previous work by the authors [6].

The numerical results obtained from the simulations allowed the adjustment of a mechanistic expression relating both thrust force and delamination factor to feed rate and cutting speed for the honed tool (see Table 5). Similar to the previous case, it is possible to generate graphics allowing prediction of the values of thrust force and delamination for a couple of cutting parameters selected (Fig. 12).

Table 6 shows the results of a set of validation experiments (cutting speed equal 50 m/min) that were performed to assess the predictability of mechanistics models previously presented. The maximum relative difference between the experimental value and the predicted value was 13.8% for the thrust force and 2.92% for the delamination, providing a good confidence level regarding the applicability of the analytical expressions.

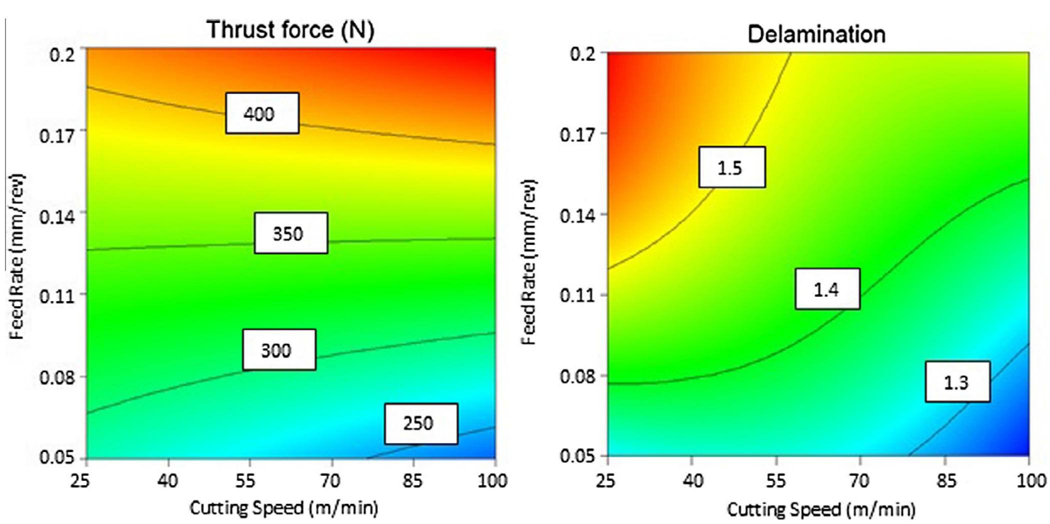

Fig. 12. Example of diagrams to estimate thrust force and delamination for honned drill bit.

Table 6
Comparison between experiments and estimated values by regression equations.

	Feed rate (mm/rev)	Thrust force			Delamination		
		Estimated	Experimental	Error (%)	Estimated	Experimental	Error (%)
Fresh drill	0.1	74.76	68.24	9.6	1.09	1.08	0.93
	0.15	84.64	74.38	13.8	1.16	1.14	1.75
Honned edge drill	0.1	313.306	358.19	12.5	1.37	1.41	2.92
	0.15	375.73	395.035	5.1	1.43	1.47	2.80

5. Conclusions

In this work, a numerical model able to predict the response of carbon/epoxy woven laminates under drilling processes has been presented. The numerical simulations predict quite faithfully the delamination damage and the thrust force; this tool has a potential use in the understanding of the interlaminar damage due to drilling in composites, allowing the reduction of experimental tests. In addition, the model is also able to estimate the thrust force and delamination damage for worn tools and complex geometries. It is possible to extend the proposed modeling scheme to new geometries and wear modes.

Validation was carried out comparing numerical results and experiments in terms of thrust force and induced delamination and good accuracy was found. The validated model was used to study the influence of different cutting parameters both in the case of new and worn tool. Clear influence of the feed rate and point angle has been observed and explained.

Finally a mechanistic model developed for rapid estimation of delamination and thrust force has been presented and validated with a very good confidence level. The expressions and surface diagrams obtained in this paper allowed prediction of thrust force and delamination once the feed rate and cutting speed are defined. This complementary analysis has elevated potential to be used in industry because of its simplicity. However it is worth noting the necessity of carry out sound previous work, both experimental and numerical, priorly required to develop these type of mechanistics models with applicability in industrial environment.

Acknowledgements

This study has been developed under the financial support of the Ministry of Economy and Competitiveness of Spain under the projects DPI2011-25999 and DPI2013-41094-R, and the FPI subprogram associated to the project DPI2011-25999 with the reference BES-2012-055162.

References

[1] Huang X. Fabrication and properties of carbon fibers. Mater 2009;2:2369–403.
[2] López de Lacalle LN, Fernández A, Olvera D, Lamikiz A, Olvera D, Rodríguez C, et al. Monitoring deep twist drilling for a rapid manufacturing of light high-strength parts. Mech Syst Sig Process 2011;25:2745–52.
[3] López de la calle LN, Lamikiz A, Campa FJ, Fdz-Valdivielso A. Design and test of a multitooth tool for CFRP milling. J Compos Mater 2009;43(26):3275–90.
[4] Liu D, Tang Y, Cong WL. A review of mechanical drilling for composite laminates. Compos Struct 2012;94:1265–79.
[5] Davim JP, Reis P. Study of delamination in drilling carbon fiber reinforced plastic (CFRP) using design experiments. Compos Struct 2003;59:481–7.
[6] Gaitonde VN, Karnik SR, Campos Rubio J, Esteves Correia A, Abrao AM, Paulo Davim J. Analysis of parametric influence on delamination in high-speed drilling of carbon fiber reinforced plastic composites. J Mater Process Technol 2008;203:431–8.
[7] Karnik SR, Gaitonde VN, Campos Rubio J, Esteves Correia A, Abrao AM, Davim JP. Delamination analysis in high speed drilling of carbon fiber reinforced plastics (CFRP) using artificial neural network model. Mater Des 2008;29:1768–76.
[8] Feito N, Díaz-Álvarez J, Díaz-Álvarez A, Cantero JL, Miguélez MH. Experimental analysis of the influence of drill point angle and wear on the drilling of woven CFRPs. Mater 2014;7:4258–71.
[9] Heisel U, Pfeifroth T. Influence of point angle on drill hole quality and machining forces when drilling CFRP. Procedia CIRP 2012;1:471.
[10] Tsao CC, Hocheng H. Taguchi analysis of delamination associated with various drill bits in drilling of composite material. Int J Mach Tools Manuf 2004;44:1085–90.
[11] Mayuet P, Gallo A, Portal A, Arroyo P, Alvarez M, Marcos M. Damaged area based study of the break-IN and break-OUT defects in the dry drilling of Carbon Fiber Reinforced Plastics (CFRP). Proc Eng 2013;63:743–51.
[12] Rawat S, Attia H. Wear mechanisms and tool life management of WC–Co drills during dry high speed drilling of woven carbon fibre composites. Wear 2009;267:1022–30.
[13] Iliescu D, Gehin D, Gutierrez ME, Girot F. Modeling and tool wear in drilling of CFRP. Int J Mach Tools Manuf 2010;50:204–13.
[14] Faraz A, Biermann D, Weinert K. Cutting edge rounding: an innovative tool wear criterion in drilling CFRP composite laminates. Int J Mach Tools Manuf 2009;49:1185–96.
[15] Chinmaya RD, Shin YC. Modeling of machining of composite materials: a review. Int J Mach Tools Manuf 2012;57:102–21.
[16] Arola D, Ramulu M. Orthogonal cutting of fiber-reinforced composites: a finite element analysis. Int J Mech Sci 1997;39:597–613.
[17] Mahdi M, Zhang L. A finite element model for the orthogonal cutting of fiber reinforced composite materials. J Mater Process Technol 2001;113:368–72.
[18] Santiuste C, Soldani X, Miguélez MH. Machining FEM model of long fiber composites for aeronautical components. Compos Struct 2010;92:691–8.
[19] Soldani X, Santiuste C, Muñoz-Sánchez A, Miguélez MH. Influence of tool geometry and numerical parameters when modeling orthogonal cutting of LFRP composites. Composites Part A 2011;42:1205–16.
[20] Santiuste C, Miguélez MH, Soldani X. Out-of-plane failure mechanisms in LFRP composite cutting. Compos Struct 2011;93:2706–13.
[21] Santiuste C, Olmedo A, Soldani X, Miguélez MH. Delamination prediction in orthogonal machining of carbon LFRP composites. J Reinf Plast Comp 2012;31(13):875–85.
[22] Durao LMP, de Moura MFSF, Marques AT. Numerical simulation of the drilling process on carbon/epoxy composite laminates. Composites Part A 2006;37:1325–33.
[23] Durao LMP, de Moura MFSF, Marques AT. Numerical prediction of delamination onset in carbon/epoxy composite laminates. Eng Fract Mech 2008;75:2767–78.
[24] Singh I, Bhatnagar N, Viswanath P. Drilling of uni directional glass fiber reinforced plastics: experimental and finite element study. Mater Des 2008;29:546–53.
[25] Upadhyay PC, Lyons JS. On the evaluation of critical thrust for delamination free drilling of composite laminates. J Reinf Plast Comp 1999;18:1287–303.
[26] Isbilir O, Ghassemieh E. Numerical investigation of the effects of drill geometry on drilling induced delamination of carbon fiber reinforced composites. Compos Struct 2013;105:126–33.
[27] Phadnis VA, Makhdum F, Roy A, Silberschmidt VV. Drilling in carbon/epoxy composites: experimental investigations and finite element implementation. Compos Part A 2013;47:41–51.
[28] Feito N, López-Puente J, Santiuste C, Miguélez MH. Numerical prediction of delamination in CFRP drilling. Compos Struct 2014;108:677–83.
[29] Varas D, Artero-Guerrero JA, Pernas-Sánchez J, López-Puente J. Analysis of high velocity impacts of steel cylinders on thin carbon/epoxy woven laminates. Compos Struct 2013;95:623–9.
[30] <http://www.guhring.com/>.
[31] Hibbit, Karlson, Sorensen Inc. ABAQUS user's manual; 2003.
[32] López-Puente J, Zaera R, Navarro C. Experimental and numerical analysis of normal and oblique ballistic impacts on thin carbon/epoxy woven laminates. Compos Part A 2008;39:374–87.